Do early diagenetic processes affect the applicability of commonly-used organic matter source tracking tools? An assessment through controlled degradation end-member mixing experiments

Morgane Derrien, Heybin Choi, Emilie Jardé, Kyung-Hoon Shin, Jin Hur

Do early diagenetic processes affect the applicability of commonly-used organic matter source tracking tools? An assessment through controlled degradation end-member mixing experiments

Morgane Derrien[a,*], Heybin Choi[b], Jardé Emilie[c], Kyung-Hoon Shin[b], and Jin Hur[a,*]

[a]*Department of Environment and Energy, Sejong University, Seoul 143-747, South Korea*

[b]*Department of Environmental Marine Sciences, Hanyang University, Ansan, Gyeonggi do 15588, South Korea*

[c] *University of Rennes 1, CNRS, Géosciences Rennes, UMR 6118, Rennes, France*

Re-submitted to *Water Research*, January 2020.

* Corresponding author

Tel. +82-2-6935-2634

E-Mail: morganederrien@sejong.ac.kr; jinhur@sejong.ac.kr

ABSTRACT

In the development of organic matter (OM) source tracking tools, it is critical to validate if (1) the tracers are conservative with source mixing, and (2) they can be conservative under diagenetic processes (e.g., microbial degradation). In this study, these two critical points were rigorously tested for three commonly-used source tracking tools (i.e., absorbance and fluorescence proxies, stable carbon isotopes and lipid biomarkers) via a controlled experiment at laboratory scale. To this end, two end-members (e.g., soil and algae), which represent the most common and contrasted sources of OM to sediments in an aquatic environment, were mixed in different ratios and then incubated under different oxygen conditions (oxic versus anoxic) in the dark at 25°C for 60 days. The initial and final signals of the source tracking tools were analyzed and compared for each mixing ratio. Based on three evaluation criteria concerning the linearity of the relationships, discrimination sensitivity, and conservative mixing behavior, we evaluated the applicability of the tools to trace the sediment organic matter in the aquatic environment. Although most of the source tracking proxies evaluated in this study showed a conservative nature after incubation, there are only a few that demonstrated both conservative behaviors with the sources mixing and under early diagenetic processes. The fluorescence proxies such as the relative distribution of a humic-like component associated with refractory source material (Ex/Em: 220/430nm), modified fluorescence index (YFI), humification index (HIX), and carbon stable isotope ratios were identified to be the most reliable tracers for tracking sedimentary OM sources under early diagenetic processes. This study provides strong insights into the validation of common OM source tracking tools for sediment and a reasonable guideline to select the optimum indices for source discrimination via end-member mixing analysis.

Keywords: Sources tracking tools; Organic matter; Sediments; Biodegradation; End-member mixing.

1.INTRODUCTION

Natural organic matter (NOM) is generated by the breakdown and degradation of organisms involving hydrosphere, biosphere, and geosphere through diverse biological, chemical, and physical processes in the natural environment (Sillanpää, 2015). NOM sources are usually classified as allochthonous or autochthonous. Allochthonous OM, which occurs from outside the aquatic environment, consists of terrigenous materials, such as vascular plants, leaves, root exudates, and soils, exported from the upstream catchment into rivers and lakes. By contrast, autochthonous OM, which is produced within water bodies, derives from aquatic biota (e.g., algae, bacteria, plankton, macrophytes, and nekton) (Derrien et al., 2019a; Volkman and Tanoue, 2002). In aquatic systems, sediments represent a large reservoir of nutrients and NOM from both inputs in various proportions (Briand et al., 2015; Fisher et al., 2005; Southwell et al., 2010; Waterson and Canuel, 2008; Zhang et al., 2009). Indeed, sedimentary OM is derived from bacteria or plankton formed in situ, but also receives allochthonous OM from the upstream catchment. Soil OM is a representative allochthonous OM source and it is easily transported into the rivers and ends up in sediments through hydrological processes (van der Meij et al., 2018). Nowadays, terrestrial organic matter input into surface waters is one of the major concerns in the context of the current climate changes as it is observed in polar regions with the release of “dormant” carbon from permafrost (Bischoff et al., 2016; Vonk et al., 2015; Wild et al., 2019). Sediments are also a reactive compartment where diagenetic processes occur inducing changes. The processes may be physical, chemical, and/or biological in nature and may occur at any time

subsequent to the arrival of a particle at the sediment-water interface (Henrichs, 1992; Kuznetsova et al., 2019; Milliken, 2003). Among the early diagenetic processes, biodegradation plays a key role as it is one of the main processes causing changes in amount, composition and properties of OM in sediment (Arndt et al., 2013; Derrien et al., 2019a; Guenet et al., 2014).

Investigating the processes that control the composition of sedimentary OM is crucial for a thorough understanding of OM dynamics and its role in the carbon cycle at a local and global scale (Gordon and Goni, 2003; Pedrosa-Pàmies et al., 2015). Identifying, apportioning and tracking the sources of OM in aquatic systems require robust, reliable and effective source tracking tools. Absorbance and fluorescence proxies, stable carbon isotopes, and lipid biomarkers are the most commonly-used OM source tracking tools in aquatic systems (Aiken, 2014; Bianchi and Canuel, 2011; Derrien et al., 2017; Meyers, 1994). These tools have been applied in diverse environments including soils, sediments, pore-water, river, lakes, and oceans for several decades (Amiotte-Suchet et al., 2007; Benner et al., 1997; Derrien et al., 2015; Fichot et al., 2013; Jaffé et al., 2004; Meyers and Ishiwatari, 1993; Toming et al., 2013; Wakeham and Canuel, 1990; Zimmerman and Canuel, 2001; Zsolnay et al., 1999). Although these tools have been used for decades, their applicability and potential limitations have not been rigorously examined yet. Nevertheless, to fully validate their use, two critical points need to be examined: 1) conservative behavior with sources mixing, and 2) conservative behavior under early diagenetic processes (e.g., microbial degradation). In our previous study, based on a simple mixing POM end-member experiment, we demonstrated that the conservative behavior of the OM source tracking tools with the mixing source is not obvious and finally raised the question of the reliability of some of the most commonly-used tools (Derrien et al., 2019b). More recently, we also investigated the biodegradation-induced changes in the porewater DOM for different

sources (Derrien et al., 2019c). The results of the latter study suggested the existence of different pathways of biodegradation with both positive and negative priming effects depending on the sources and the ratio of labile material. All these observations clearly justify the questioning of the applicability to these tools in natural systems and the necessity to test them for both criteria.

In this context, we designed a controlled degradation experiment at laboratory scale using organic-rich sediments artificially composed of two contrasting OM end-members (i.e., soil and algae) at known mixing ratios. The incubations were performed under oxic and anoxic conditions in order to reproduce different configurations of natural sediment (Kristensen, 2000). Hence, this study aimed to establish the applicability of 3 commonly-used source tracking tools (i.e., absorbance and fluorescence proxies, stable carbon isotopes, and lipid biomarkers) during early diagenetic processes in the natural environment. As a result, the specific objectives of this study were (i) to study the influence of oxygen on the degradation-induced changes, and (ii) to examine the conservative/non conservative behaviors of the three source discrimination tools in artificial sediments before and after biodegradation, and (iii) to evaluate the conservative/non conservative behaviors of the three source discrimination tools with sources mixing in the artificial sediments.

2. MATERIAL AND METHODS

2.1. Experimental design of the incubation experiment

Two end-members (i.e., soil and algae), as the major organic sources of sediments, were mixed at soil to algae ratios of 100:0, 75:25, 50:50, 25:75, and 0:100, respectively, on the basis of organic carbon (OC) concentrations, not their masses, after the OC contents of the two end-members were taken into account. Briefly, a topsoil (0-10cm) sample was collected as the soil

115 end-member at Bukhansan National Park (37°43’37.0” N 127°00’50.9”) in South Korea. A
116 commercial unicellular green alga (*Chlorella vulgaris*), which is commonly found in lakes and
117 ponds in South Korea, was purchased as the algae end-member from Aquanet Co., Ltd. in
118 Gyeongsangnam-do, South Korea. Detailed information on the two end-members can be found
119 in Derrien et al., 2019b.

120 Incubation experiments in oxic and anoxic conditions were performed in pre-washed and
121 pre-combusted (450°C for 4 hours) 125 ml Wheaton® amber glass bottles with Teflon
122 screwcaps. Samples for anoxic incubation were prepared and sampled using sterile Aldrich®
123 AtmosBag two-hand glove bag. A mass (12 g) of the end-member mixture samples were mixed
124 with ultrapure water (Barnstead™ Easypure™ RoDi, Thermo Scientific) at a solid to solution
125 ratio of 1:4 and equilibrated for 48 h in the dark at room temperature after shaking at 100 rpm for
126 one hour. River water from Jungnang river in Seoul (37° 40′ 16″N, 127° 04′ 47″E) was used as
127 inoculum for microbial incubation. The collected river water sample was first passed through a
128 GF/C (pre-combusted, 1.2 μm pore-sized) and 10 mM of inorganic nutrients (NH_4NO_3 and
129 K_2HPO_4) was added to the filtered river water for sufficient microbial growth. Then, the
130 inoculum solution was covered by aluminum foil to protect the solution from light to avoid the
131 growth of algae and finally kept at room temperature under slow shaking (80 rpm) for 2 days.
132 Prior to incubation, all artificial sediment samples were spiked with 3% (v/v) of the prepared
133 inoculum, and a sufficient amount (1%, v/v) of nutrients (NH_4NO_3 and K_2HPO_4 at 10 mM) was
134 added to each sample to avoid nutrient limitations during the incubation. Finally, the samples in
135 oxic and anoxic conditions were incubated in the dark at 25°C for 60 days (Guenet et al., 2014;
136 Navel et al., 2012). No control was prepared because it required the poisoning of the samples
137 with either mercuric chloride or sodium azide, which are extremely toxic and environmentally

harmful and more importantly result in fluorescence quenching (Park and Snyder, 2018; Retelletti Brogi et al., 2019). Samples under oxic conditions were aerated every 3 days under a fume hood in order to minimize the contamination by microorganisms in the air. Samples were sacrificed for sampling on day 0 and day 60, with "day 0" corresponding to the day when the samples were inoculated. The degradation experiments were carried out in duplicate.

The sampling was performed according to the following. First, samples were taken from the incubator and the overlying water was carefully removed not to disturb the sediment. The artificial sediment samples were then centrifuged at 5000 rpm for 20 min to remove the porewater. Finally, the porewater-free sediment samples were freeze-dried, ground, and homogenized for further analyses.

2.2. Spectroscopic measurements

To investigate the absorbance and fluorescence properties of the artificial sediment, it is necessary to perform an extraction of the OM (e.g., extraction of the dissolved OM from the sedimentary OM). Extraction can be performed with different solvents. According to our previous results comparing common solvent-based OM extraction methods, the water extraction was identified as the preferred extraction method for the application of the spectroscopic tool to POM source discrimination (Derrien et al., 2019b). In this study, the same procedure was used to obtain the water-extractable organic matter (WEOM) of the artificial sediment samples.

The dissolved organic carbon (DOC) concentrations were measured using a Shimadzu V-CPH TOC analyzer. The absorption spectra were scanned from 200 to 800 nm at 0.5 nm-interval using an ultraviolet-visible (UV-vis) spectrometer (Shimadzu UV-1300). The fluorescence excitation-emission matrices (EEMs) were obtained with a luminescence spectrometer (Hitachi

F7000, Japan) following the procedure previously described by Retelletti Brogi et al. (2019). A total of 82 EEMs were collected for the PARAFAC modeling, and it was processed using MATLAB R2013b (Mathworks, USA) with the drEEM toolbox (Murphy et al., 2013). The validation of the PARAFAC model was made by split-half analysis and percentage of explained variance (>99.5%). By using corrected EEMs, several classical fluorescence indices (e.g., fluorescence index and modified fluorescence index: FI and YFI, the humification index: HIX, and the index of recent autochthonous contribution BIX) were calculated (Heo et al., 2016; Huguet et al., 2009; Zsolnay et al., 1999). The maximum fluorescence intensities (F_{max}) of the identified PARAFAC components were used to represent their relative abundance (%).

2.3. Carbon and nitrogen stable isotope ratio analyses

Before carbon stable isotope analysis, inorganic carbon was removed by 1N HCl treatment, whereas untreated samples were directly used for the nitrogen isotope ratio analysis (Carabel et al., 2006). The total organic carbon (TOC) and the carbon stable isotope ratio ($\delta^{13}C$) were measured using an elemental analyzer that was coupled with an isotope ratio mass spectrometer (EA-IRMS; EuroEA-Isoprime IRMS, GV Instruments, UK). Stable isotope ratios were calculated using the standard d notation:

$$\delta^{13}C(‰) = \left((R_{sample}/R_{Reference}) - 1\right) \times 1000 \quad (1)$$

where R is the corresponding ratio of $^{13}C/^{12}C$. The standard reference material was IAEA-CH-3, Cellulose ($\delta^{13}C$ = -24.724 ± 0.041 (vs VPDB, Vienna Pee Dee Belemnite)). The analytical precision was 0.05‰.

2.4. The sterols/stanols analysis

The total lipid fraction of the artificial sediments was extracted with dichloromethane using an accelerated solvent extractor (ASE 200, Dionex). Conditions of the extraction are described in Derrien et al. (2011). The total lipid extract was then fractionated using solid/liquid chromatography (silica column) to isolate the polar fraction. The polar fraction was derivatized with a mixture of N,O-bis-(trimethylsilyl)trifluoroacetamide and trimethylchloro-silane (BSTFA + TMCS, 99/1, v/v, Supelco) after addition of 5α-cholestane (CDN isotope) as an internal standard (IS). Derivatized samples were analyzed by gas chromatography-mass spectrometry (GC–MS) using a Shimadzu QP2010plus equipped with a capillary column (Supelco, 60m×0.25mm ID, 0.25 µm film thickness). The temperature of the transfer line was set at 280°C, and molecules were ionized by electron impact using the energy of 70 eV. The temperature of the ionization source was set at 200°C. Samples were injected in splitless mode at 310°C. The oven temperature was programmed from an initial temperature of 200°C (held for 1 min) then rising to 310°C at 15°C/min (held for 35 min). Helium was used as the carrier gas, with a flow rate of 1.0 mL/min. The analyses were made in selective ion monitoring mode (SIM). The compound identification was performed based on the comparison of the retention times and the mass spectra with the available standards or the literature data (Table S1) (Debieu et al., 1992; Derrien et al., 2019b; Harrault et al., 2019). The quantification was achieved with a 5-point internal calibration curve (two series of calibration solutions: 0.1, 0.3, 0.5, 0.7 and 1ppm or 1, 3, 5, 7, and 10 ppm) of sterol and stanol standards with a constant IS concentration at 0.5 or 5 ppm, respectively.

2.6. Conservative mixing relationship and statistical analyses

In order to assess the applicability of the different source tracking tools during early diagenetic processes, several evaluation criteria were established, which were already presented and used in a previous study (Derrien et al., 2019b). First, the linearity of the measured parameters in artificial sediments was examined with respect to the increasing abundance of one end-member (e.g., soil or algae). The relationship was considered "linear" for a high coefficient of determination $R^2 > 0.8$ and an associated p-value < 0.01. Then, the regression slope of the measured values (Sm) normalized by the standard deviation of the measurement (Sm/SD) was used to evaluate the sensitivity of the source discrimination. A value of the Sm/SD ≥ 0.5 was considered as an acceptable range for the sensitivity regarding the source discrimination relative to the measurement uncertainty. Finally, the deviation from the ideal values for a conservative mixing relationship was estimated in calculating the percent difference (%difference) between the slopes for the measured (Sm) and the predicted (Sp) values. The predicted values were calculated using the pure end member's values and the mixing ratios under a linear conservative mixing assumption (Table S2). A %difference of < 10% was considered to be an acceptable degree of the deviation for the conservative mixing relationship.

3.RESULTS AND DISCUSSION

3.1. Spectroscopic indices

3.1.1. Identification of different fluorescent components via EEM-PARAFAC

Four different components were identified, which included two humic-like components (C1 and C2) and two protein-like components (C3 and C4) (Fig. S1). All the identified components were consistent with those previously reported and/or matched well with the Open Fluor database with similarity scores > 0.95 (Table S3). Component 1 (C1), which had a

maximum at 220/430 nm (Ex/Em), can be assigned to a typical terrestrial humic-like component (Graeber et al., 2012; Retelletti Brogi et al., 2019b; Yamashita et al., 2010). Component 2 (C2), which exhibited the maxima at 220/547 nm (Ex/Em) can be associated with a humic-like component or aromatic conjugated macromolecular substances of terrestrial origin (Galletti et al., 2019; Osburn et al., 2016b; Wünsch et al., 2017). Component 3 (C3, peaked at 220,265/361 nm (Ex/Em)) and component 4 (C4, peaked at 220/309 nm (Ex/Em)) were reported as protein-like substances, namely tryptophan-like and tyrosine-like components, respectively (Cawley et al., 2012; D'Andrilli et al., 2017; Derrien et al., 2019c; Yamashita et al., 2013).

3.1.2. Changes in the absorbance and fluorescence proxies of the end-members after incubation

The original (at 0-day of incubation) spectroscopic characteristics of the end-members for this study were consistent with those reported in our previous study (Derrien et al., 2019b) (Table 1). Briefly, the soil end-member was mainly characterized by a high abundance of both humic-like components, C1 and C2, with the percentages of > 47% and > 34%, respectively. On the contrary, the algae end-member consisted only of the two protein-like components, C3 and C4, in equal proportions. Higher values of $SUVA_{254}$ (> 2 $L.mg^{-1}.m^{-1}$) and HIX (> 15) were observed for the soil end-member corroborating the high content of humic substances (Derrien et al., 2017; Zsolnay et al., 1999) while higher values of YFI (>3.5) and BIX (>1) were for the algae end-member reflecting its allochthonous origin (Heo et al., 2016; Huguet et al., 2009).

The biodegradation led to changes in most of the spectroscopic parameters for both end-members (Table 1). Although there were some differences between the two oxygen conditions, these differences were not statistically significant as the p-values were > 0.95 (e.g., 0.95 and 0.99 for soil and algae end-members, respectively). After 60 days of incubation, the soil end member

exhibited a partial (~30%) to complete decrease in the abundance for both protein-like components (C3 and C4). For the main fluorescent components, biodegradation induced a slight depletion of the component C1 (< 10%) while the second humic-like component (C2) became more enriched by 20 to 30 %. Regarding the spectroscopic indices, substantial changes were mainly observed for HIX with an increase of the value from 16.9 ± 0.7 to 21.3 ± 0.2 under oxic conditions. However, the increase was slight under anoxic conditions. These results suggest the initial consumption of labile substances as reflected by the partial to complete consumption of the two protein-like components, and a production of high molecular weight and aromatic substances (C2) through the alteration of existing compounds (C1) and/or the production of new compounds by autotrophic organisms (Derrien et al., 2019a; Hansen et al., 2016; Kinsey et al., 2018).

The algae end member also displayed biodegradation-induced changes in the spectroscopic parameters. The most notable change was the decrease in the relative abundance of the C3 component (i.e., %C3) changing from 46.0 ± 0.8 to 42.4 ± 1.1% in parallel to the increase of the %C4 values from 52.5 ± 0.6 to 56.5 ± 1.1%. The two fluorescence indices, FI and YFI, showed an increasing trend over incubation, with highest increasing trend for FI under oxic conditions (0.7 ± 0.0 to 1.0 ± 0.0) and YFI under anoxic conditions (3.6 ± 0.0 to 4.1 ± 0.0). The rest of the indices exhibited little to slight changes in the values specifically under anoxic conditions. For instance, BIX presented an increase of ~20% after incubation under anoxic conditions compared to 3% under oxic conditions. Although the results could be apparently interpreted as the occurrence of a potential effect of the oxygen condition, the t-test demonstrated that these changes were not significant enough (p-values >0.95). These observations suggest that the

biodegradation-induced changes in the spectroscopic source indices were less pronounced for the algae end-member than for the soil counterpart.

3.1.3. Biodegradation-induced deviations from a relationships

Biodegradation-induced changes in the absorbance and fluorescence proxies with the increasing of the algal content in the artificial sediments are shown in Figs. 1 and 2. The oxygen condition does not seem to be a critical factor for the biodegradation-induced changes as the results were similar between the oxic and anoxic conditions (p-value of >0.96). The trends of the proxies at 0 day and 60 days of incubation (i.e., %C1, %C2, YFI, HIX, and BIX; Fig. 1 and Fig. 2c, d, e) with increasing algal content in the mixture mostly remained the same (p-values > 0.6 for each proxy), which demonstrates a minor effect of the degradation on the changing trends of the signals with source mixing. By contrast, deviations between both incubation times were observed for the proxies including %C3, %C4, $SUVA_{254}$, and FI. $SUVA_{254}$ and FI (Fig 1 and Fig 2a, b) displayed a deviation after biodegradation along with the increase of the algae fraction except for the mixing ratio soil/algae 25/75. However, for %C3 and %C4, the deviation is the most pronounced at the particular mixing ratio (i.e., 25/75).

In order to evaluate the applicability of spectroscopic indices to identify OM sources during early diagenesis, the initial relationships between the absorbance/fluorescence proxies and the abundance of algal content in the mixture were investigated (Table 2) and then compared to the relationship after the biodegradation (Table 3). At 0-day of incubation (Table 2), only %C1, %C2, %C4, and $SUVA_{254}$ satisfied the threshold values of the three evaluation criteria (i.e., R^2 with p-value < 0.01, Sm/SD > 0.5, and % difference > 10%) for one (e.g. %C2 and $SUVA_{254}$) or both of the oxygen conditions (e.g. %C1 and %C4). The parameters of YFI and HIX can also be

296 suggested as good indices in terms of the relationship linearity as they meet 2 out of the 3 criteria
297 without any effect of the oxygen condition, while %C3 and FI seem to be reliable indices for
298 anoxic and oxic conditions, respectively. BIX does not validate any of the criteria. Among these
299 spectroscopic indices, after incubation, only %C1, YFI and HIX still satisfied all the evaluation
300 criteria for both oxygen conditions after biodegradation except HIX under anoxic condition
301 which did not validate the sensitivity criterion (S_m/SD = 0.169) (Table 3). The other indices
302 failed to meet the criteria in terms of linearity, sensitivity and exhibited a higher degree of the
303 deviation from the ideal end-member mixing ratios (i.e., %C3, %C4, $SUVA_{254}$, FI) after
304 microbial degradation. The non-conservative behavior of the latter indices is probably related to
305 the labile characteristic of these compounds (protein-like). From the comparison of all
306 spectroscopic proxies using the evaluation criteria at 0-day and 60-days incubation, it can be
307 concluded that the relative abundance of C1 and the two fluorescence indices, YFI and HIX,
308 represent the optimum fluorescence proxies for the OM source discrimination with varying end-
309 member mixing ratios.
310
311 **3.2. Carbon isotope ratios**
312 3.2.1. Changes for carbon isotope ratios of the end-members after incubation
313 As has been found for the spectroscopic characteristics, the isotope results of the end-
314 members at 0-day of incubation were similar to those reported in our previous study (Derrien et
315 al., 2019b) and in lines with other literature (Pardue et al., 1976; Yu et al., 2015). The values for
316 the soil end-member were -27.2 ± 0.1‰ (oxic) and -26.7 ± 0.1‰ (anoxic), while those of the
317 algae end-member were -11.9 ± 0.0‰ (oxic) and -11.4 ± 0.1‰ (anoxic).

After incubation, the values of each end-member remained invariant suggesting no effect of the biodegradation on the carbon isotopic composition. In addition, no significant difference was observed between the two oxygen conditions as the p-values were >0.3 and >0.9 for soil and algae end-members, respectively. These results confirm the chemical stability of the $\delta^{13}C$ to trace the sedimentary OM under the early diagenetic processes irrespective of oxygen presence.

3.2.2. Biodegradation-induced deviations from end member mixing analysis (EMMA) relationships

Biodegradation-induced changes in the $\delta^{13}C$ values of the artificial sediment mixtures with the increase of the algal content are shown in Fig. 3. The variation of the $\delta^{13}C$ values exhibited a linear relationship with the increase of the algal end member fraction both before and after biodegradation (Tables 2 and 3). In addition, the trend of the carbon stable isotope with increasing algal content in the mixture mostly remained the same before and after 60-days of incubation, demonstrating the resistance to isotopic alteration of $\delta^{13}C$ during sedimentary diagenesis. However, a deviation was exceptionally noted for a mixing ratio with an equal proportion of both end-members (soil/algae, 50/50). The decomposition of OM, mediated by a variety of microbial processes, can progressively modify the bulk composition of the organic substrates because different OM fractions do not have the same degradation rate (Lehmann et al., 2002; Meyers, 1994). Such selective losses of certain OM fractions may lead to a diagenetic shift in $\delta^{13}C$ (Benner et al., 1997; Harvey et al., 1995), leaving irreversible changes in the original signature. This is probably what was observed in this present study for the 50/50 artificial sediment mixture. Although the stable isotopes are widely recognized as a reliable and robust tool to trace sediment OM sources and their linear and conservative behavior in a context of

341 artificial end-member mixing (Derrien et al., 2019b), their specificity to individual sources might
342 be weakened by early diagenesis of sediments (Bianchi and Canuel, 2011; Xiao and Liu, 2010).
343 Despite this slight deviation, the $\delta^{13}C$ tool satisfied the three (and 2 for anoxic condition)
344 established criteria (e.g., linearity, sensitivity, and deviation), evidencing its linear conservative
345 mixing behavior after biodegradation, with the R^2 values ranging from 0.969 (oxic) and 0.898
346 (anoxic) with the p-values of ≤ 0.01, %difference of <10% and a sensitivity Sm/SD of 1.431
347 (oxic condition) (Table 3). These results clearly demonstrate the robustness and reliability of the
348 $\delta^{13}C$ tool for source discrimination of the sedimentary OM even after diagenetic processes.
349
350 **3.3. Sterols/stanols biomarkers**
351 3.3.1. Changes in the sterol/stanols distributions of the end-members after incubation
352 The original (at 0-day of incubation) biomarker distribution of the end-members for this
353 study was consistent with those reported in our previous study (Derrien et al., 2019b). Briefly,
354 the soil end member was characterized by abundant amounts (> 80%) of terrestrial sterols, such
355 as sitosterol, stigmasterol, and campesterol (Table 1), which agreed with the previous literature
356 (Bouloubassi et al., 1997; Derrien et al., 2011; Volkman, 2005). Fecosterol, a fungi or lichens
357 sterol biomarker (Debieu et al., 1992), sitostanol (i.e., a by-product of sitosterol) and cholesterol,
358 the most ubiquitous sterol (Leeming and Nichols, 1998), contributed <10% of the total
359 sterol/stanol distribution. Unlike the soil end-member, the algae was characterized by a high
360 abundance (>70%) of ergosterol (i.e., a green algae sterol biomarker) and the occurrence of
361 sitosterol and cholesterol, which corresponded to ~18% and ~5% of the sterol compounds in the
362 distribution, respectively.

After biodegradation, the distribution in sterols/stanols in the end-members remained the same, suggesting no effect of biodegradation such as it was observed for the carbon isotopic composition. Likewise, no significant difference was observed between the two oxygen conditions with the p-values of > 0.90 for both end-members. These results confirm the chemical stability of the biomarkers to trace the sedimentary OM sources under 60 days of diagenesis dominated by biodegradation.

3.3.2. Biodegradation-induced deviations from EMMA relationships

Biodegradation-induced changes in the distribution of sterol/stanol biomarkers in the artificial sediments with increasing algal content are shown in Fig. 4. In most cases, the oxygen condition does not seem to be a critical factor for the biodegradation-induced changes, which was observed for all the biomarkers (p-value >0.99). For all the biomarkers, the observed distribution values at all varying algal content between 0-day and 60-days of incubation were the same based on paired t-test (p-value > 0.5). These observations demonstrate the chemical stability of these lipid biomarkers to biodegradation-induced alterations.

Regarding the applicability of the lipid biomarker to identify the source of the sedimentary OM during early diagenesis, none of them satisfy the established evaluation criteria either at 0-day or 60-days of incubation (Table 2 and 3). Surprisingly, the source-specific biomarkers, found only in one of the two end-members (Table 1) such as ergosterol, fecosterol, campesterol, stigmasterol or sitostanol, even did not follow a conservative behavior with sources mixing before biodegradation as the highest R^2 were still < 0.8 with p-values > 0.05. For example, campesterol, presented a R^2 of 0.695 with a p-values of 0.079 and 0.722 (p-value=0.068) in oxic and anoxic conditions, respectively (Table 2). It is noteworthy that

biodegradation-induces changes on the sitostanol resulted in improved linearity criterion with the R^2 values changing from 0.530 (0.163) to 0.638 (0.105) and 0.544 (0.155) to 0.723 (0.068) for 0-day and 60-days of incubation, respectively and specifically the reduction in the deviation under anoxic condition (i.e., 11.8% to 6.2%). This singular behavior can be related to the nature of the by-products of the biomarker showing a higher sensitivity to microbial alterations (Bull et al., 2002). On the other hand, the incapability of the sterols and stanols lipid biomarker to reflect a conservative behavior with sources mixing was already suggested by previous studies (Derrien et al., 2019b; Shah et al., 2007). Nevertheless, it is noteworthy to observe the conservative behavior of these lipid biomarkers under early diagenetic processes.

3.4. Implications for the applicability of the organic matter source tracking tools

In this study, the discrimination capacities of the commonly used source tracking tools during biodegradation were evaluated and compared using artificial sediments with different mixing ratios of two contrasting OM sources. Two modes were observed: (i) conservative behavior in terms of both sources mixing and biodegradation and (ii) single conservative behavior in terms of biodegradation only. The results of this study demonstrated the strong capacity and the robustness of the carbon stable isotope ratios to identify and estimate the source contribution in artificial sediment mixtures under diagenesis processes. Several spectroscopic indices, such as the relative distribution of the specific fluorescent components (i.e., C1: typical terrestrial humic-like component), YFI, and HIX also represent a robust source tracking tools that were applicable for source apportionment to the artificial sediment mixtures samples under the influence of biodegradation. Regrettably, the lipid biomarkers failed in source apportionment in the artificial sediment mixtures. However, they demonstrated a resistance to microbial

409 alterations in time. Regarding the oxygen conditions, this study provides, for the first time, clear
410 evidence of little to slight effect on the efficacy of the 3 tested sources tracking tools in artificial
411 sediment mixtures.

412 All of these tools were widely utilized to track and estimate OM sources in various
413 aquatic environments, including rivers, groundwater, lakes, coastal area and oceans (Affouri and
414 Sahraoui, 2017; Derrien et al., 2018; Li et al., 2015; Ogrinc et al., 2005; Osburn et al., 2016a;
415 Toming et al., 2013; Zhang et al., 2017). They were used with the assumption of a conservative
416 mixing behavior and stability under diagenetic processes without firstly evaluating the potential
417 limited applicability. But this study provides strong evidence that the application of these
418 commonly-used tools for OM source tracking could lead to a disruption of the source assignment
419 to a wrong estimation of OM source contribution in the context of early diagenesis. Aside from
420 demonstrating a certain weakness to a complete failure of some of the commonly-used source
421 tracking tools to identify and estimate OM source contribution, this study also raises the question
422 of temporal scale. 60 days of incubation correspond to a short period of time at the diagenesis
423 scale. Therefore, it is reasonable to presume that in higher temporal scale, the limitations of the
424 tools may increase to reach the point where the source tracking tools will not be sustainable
425 anymore, leading to misinterpretations of the biogeochemical processes and dynamics of the OM
426 in specific environments.

427 Experiments carried out under controlled conditions can help in identifying the effects
428 that certain factors have on OM dynamics and properties by excluding any interferences that
429 might exist in real environments (Derrien et al., 2019a). In the present case, we tried to elucidate
430 the combined effect of multiple factors (i.e., microbial degradation, mixing sources ratios and
431 oxygen condition). Although the results of this study provide significant insights for the

characterization of the OM and more generally for the biogeosciences field, it is necessary to be aware of some limitations of this kind of approach (i.e., a limited number of OM sources (i.e., soil and algae) and choice of the degradation time). Nevertheless, in this current framework, carbon stable isotope ratios, the relative distribution of refractory material fluorescent component, YFI and HIX indices could be suggested as a reasonable tracer with the most conservative behavior and the highest sensitivity to source discrimination in the period of early diagenesis.

4. CONCLUSION

The applicability of three commonly-used source tracking tools (i.e., fluorescence proxies, carbon stable isotope ratios, and lipid biomarkers) was tested on artificial sediments of different mixing ratios of two contrasting OM sources and after biodegradation for both oxygen conditions (i.e., oxic and anoxic). Based on three evaluation criteria concerning the linearity of the relationships, the discrimination sensitivity, and the conservative mixing behavior, the following conclusions can be drawn:

- The oxygen condition seems to make a limited contribution to biodegradation-induced changes by comparing initial and final tested properties after 60 days of degradation.
- Most of the sources tracking proxies evaluated in this study show a conservative behavior with respect to biodegradation. By contrast, only a few demonstrated a linear relationship with the increasing portion of one end-members in the mixtures.
- The fluorescence proxies such as the relative distribution of a humic-like component associated with refractory source material (C1, Ex/Em: 220/430nm), YFI, and HIX indices were found to be reliable proxies for source tracking after biodegradation.

- Carbon stable isotope ratios exhibited a linear conservative relationship with varying mixing ratios of end members before and after biodegradation, demonstrating its strong capacity for identifying the source's contribution at any time under diagenesis.
- The biomarkers of sterols/stanols did show a conservative nature under biodegradation however they did not present a good linear and conservative behavior with varying mixing ratios of end members.

Although these results clearly demonstrate the sensitivity to early diagenesis processes to most of the commonly used sources tracking tools, further studies need to be performed to rigorously evaluate the effects of the incubation time, temperature, sediment depth to fully validate these results.

Acknowledgments

This work was supported by the National Research Foundation of Korea (NRF) grants and was funded by the Korean government (MSIP) (No. 2017R1A4A1015393 and 2017R1D1A1B033546).

References

Affouri, H., Sahraoui, O., 2017. The sedimentary organic matter from a Lake Ichkeul core (far northern Tunisia): Rock-Eval and biomarker approach. J. African Earth Sci. 129, 248–259. https://doi.org/10.1016/j.jafrearsci.2017.01.017

Aiken, G., 2014. Fluorescence and Dissolved Organic Matter, in: Baker, A., Reynolds, D.M., Lead, J., Coble, P.G., Spencer, R.G.M. (Eds.), Aquatic Organic Matter Fluorescence. Cambridge University Press, Cambridge, pp. 35–74. https://doi.org/DOI:

10.1017/CBO9781139045452.005

Amiotte-Suchet, P., Linglois, N., Leveque, J., Andreux, F., 2007. 13C composition of dissolved organic carbon in upland forested catchments of the Morvan Mountains (France): Influence of coniferous and deciduous vegetation. J. Hydrol. 335, 354–363. https://doi.org/http://dx.doi.org/10.1016/j.jhydrol.2006.12.002

Arndt, S., Jørgensen, B.B., LaRowe, D.E., Middelburg, J.J., Pancost, R.D., Regnier, P., 2013. Quantifying the degradation of organic matter in marine sediments: A review and synthesis. Earth-Science Rev. 123, 53–86. https://doi.org/10.1016/J.EARSCIREV.2013.02.008

Benner, R., Biddanda, B., Black, B., McCarthy, M., 1997. Abundance, size distribution, and stable carbon and nitrogen isotopic compositions of marine organic matter isolated by tangential-flow ultrafiltration. Mar. Chem. 57, 243–263. https://doi.org/http://dx.doi.org/10.1016/S0304-4203(97)00013-3

Bianchi, T.S., Canuel, E.A., 2011. Chemical Biomarkers in Aquatic Ecosystems. Princeton University Press, Princeton University.

Bischoff, J., Sparkes, R.B., Doğrul Selver, A., Spencer, R.G.M., Gustafsson, Ö., Semiletov, I.P., Dudarev, O. V., Wagner, D., Rivkina, E., van Dongen, B.E., Talbot, H.M., 2016. Source, transport and fate of soil organic matter inferred from microbial biomarker lipids on the East Siberian Arctic Shelf. Biogeosciences 13, 4899–4914. https://doi.org/10.5194/bg-13-4899-2016

Bouloubassi, I., Lipiatou, E., Saliot, A., Tolosa, I., Bayona, J.M.M., Albaigés, J., 1997. Carbon sources and cycle in the western Mediterranean—the use of molecular markers to determine the origin of organic matter. Deep Sea Res. Part II Top. Stud. Oceanogr. 44, 781–799. https://doi.org/https://doi.org/10.1016/S0967-0645(96)00094-X

Briand, M.J., Bonnet, X., Goiran, C., Guillou, G., Letourneur, Y., 2015. Major Sources of Organic Matter in a Complex Coral Reef Lagoon: Identification from Isotopic Signatures (δ(13)C and δ(15)N). PLoS One 10, e0131555. https://doi.org/10.1371/journal.pone.0131555

Bull, I.D., Lockheart, M.J., Elhmmali, M.M., Roberts, D.J., Evershed, R.P., 2002. The origin of faeces by means of biomarker detection. Environ. Int. 27, 647–654.

Carabel, S., Godínez-Domínguez, E., Verísimo, P., Fernández, L., Freire, J., 2006. An assessment of sample processing methods for stable isotope analyses of marine food webs. J. Exp. Mar. Bio. Ecol. 336, 254–261. https://doi.org/http://dx.doi.org/10.1016/j.jembe.2006.06.001

Cawley, K.M., Ding, Y., Fourqurean, J., Jaffé, R., 2012. Characterising the sources and fate of dissolved organic matter in Shark Bay, Australia: a preliminary study using optical properties and stable carbon isotopes. Mar. Freshw. Res. 63, 1098–1107. https://doi.org/https://doi.org/10.1071/MF12028

D'Andrilli, J., Foreman, C.M., Sigl, M., Priscu, J.C., McConnell, J.R., 2017. A 21 000-year record of fluorescent organic matter markers in the WAIS Divide ice core. Clim. Past 13, 533–544.

Debieu, D., Gall, C., Gredt, M., Bach, J., Malosse, C., Leroux, P., 1992. Ergosterol biosynthesis and its inhibition by fenpropimorph in Fusarium species. Phytochemistry 31, 1223–1233. https://doi.org/https://doi.org/10.1016/0031-9422(92)80265-G

Derrien, M., Brogi, S.R., Gonçalves-Araujo, R., Retelletti Brogi, S., Gonçalves-Araujo, R., 2019a. Characterization of aquatic organic matter: Assessment, perspectives and research priorities. Water Res. 163, 114908. https://doi.org/10.1016/J.WATRES.2019.114908

523 Derrien, M., Cabrera, F.A., Tavera, N.L.V., Kantún Manzano, C.A., Vizcaino, S.C., 2015.
524 Sources and distribution of organic matter along the Ring of Cenotes, Yucatan, Mexico:
525 Sterol markers and statistical approaches. Sci. Total Environ. 511.
526 https://doi.org/10.1016/j.scitotenv.2014.12.053
527 Derrien, M., Jardé, E., Gruau, G., Pierson-Wickmann, A.-C., 2011. Extreme variability of steroid
528 profiles in cow feces and pig slurries at the regional scale: Implications for the use of
529 steroids to specify fecal pollution sources in waters. J. Agric. Food Chem. 59.
530 https://doi.org/10.1021/jf201040v
531 Derrien, M., Kim, M.S., Ock, G., Hong, S., Cho, J., Shin, K.H.K.-H.K.H., Hur, J., 2018.
532 Estimation of different source contributions to sediment organic matter in an agricultural-
533 forested watershed using end member mixing analyses based on stable isotope ratios and
534 fluorescence spectroscopy. Sci. Total Environ. 618, 569–578.
535 https://doi.org/https://doi.org/10.1016/j.scitotenv.2017.11.067
536 Derrien, M., Shin, K.-H., Hur, J., 2019b. Assessment on applicability of common source tracking
537 tools for particulate organic matter in controlled end member mixing experiments. Sci.
538 Total Environ. 666, 187–196. https://doi.org/10.1016/j.scitotenv.2019.02.258
539 Derrien, M., Shin, K.-H., Hur, J., 2019c. Biodegradation-induced signatures in sediment pore
540 water dissolved organic matter: Implications from artificial sediments composed of two
541 contrasting sources. Sci. Total Environ. 694, 133714.
542 Derrien, M., Yang, L., Hur, J., 2017. Lipid biomarkers and spectroscopic indices for identifying
543 organic matter sources in aquatic environments: A review. Water Res. 112.
544 https://doi.org/10.1016/j.watres.2017.01.023
545 Fichot, C.G., Kaiser, K., Hooker, S.B., Amon, R.M.W., Babin, M., Bélanger, S., Walker, S.A.,

546 Benner, R., 2013. Pan-Arctic distributions of continental runoff in the Arctic Ocean 3, 1053.
547 https://doi.org/10.1038/srep01053http://dharmasastra.live.cf.private.springer.com/articles/sr
548 ep01053#supplementary-information
549 Fisher, M.M., Reddy, K.R., James, R.T., 2005. Internal nutrient loads from sediments in a
550 shallow, subtropical lake. Lake Reserv. Manag. 21, 338–349.
551 https://doi.org/10.1080/07438140509354439
552 Galletti, Y., Gonnelli, M., Retelletti Brogi, S., Vestri, S., Santinelli, C., 2019. DOM dynamics in
553 open waters of the Mediterranean Sea: New insights from optical properties. Deep. Res.
554 Part I Oceanogr. Res. Pap. 144, 95–114. https://doi.org/10.1016/j.dsr.2019.01.007
555 Gordon, E.S., Goni, M.A., 2003. Sources and distribution of terrigenous organic matter delivered
556 by the Atchafalaya River to sediments in the northern Gulf of Mexico. Geochim.
557 Cosmochim. Acta 67, 2359–2375. https://doi.org/10.1016/S0016-7037(02)01412-6
558 Graeber, D., Gelbrecht, J., Pusch, M.T., Anlanger, C., von Schiller, D., 2012. Agriculture has
559 changed the amount and composition of dissolved organic matter in Central European
560 headwater streams. Sci. Total Environ. 438, 435–446.
561 https://doi.org/https://doi.org/10.1016/j.scitotenv.2012.08.087
562 Guenet, B., Danger, M., Harrault, L., Allard, B., Jauset-Alcala, M., Bardoux, G., Benest, D.,
563 Abbadie, L., Lacroix, G., 2014. Fast mineralization of land-born C in inland waters: first
564 experimental evidences of aquatic priming effect. Hydrobiologia 721, 35–44.
565 https://doi.org/10.1007/s10750-013-1635-1
566 Hansen, A.M., Kraus, T.E.C., Pellerin, B.A., Fleck, J.A., Downing, B.D., Bergamaschi, B.A.,
567 2016. Optical properties of dissolved organic matter (DOM): Effects of biological and
568 photolytic degradation. Limnol. Oceanogr. 61, 1015–1032.

https://doi.org/10.1002/lno.10270

Harrault, L., Milek, K., Jardé, E., Jeanneau, L., Derrien, M., Anderson, D.G., 2019. Faecal biomarkers can distinguish specific mammalian species in modern and past environments. PLoS One 14, e0211119. https://doi.org/10.1371/journal.pone.0211119

Harvey, R.H., Tuttle, J.H., Bell, T.J., 1995. Kinetics of phytoplankton decay during simulated sedimentation: Changes in biochemical composition and microbial activity under oxic and anoxic conditions. Geochim. Cosmochim. Acta 59, 3367–3377. https://doi.org/http://dx.doi.org/10.1016/0016-7037(95)00217-N

Henrichs, S.M., 1992. Early diagenesis of organic matter in marine sediments: progress and perplexity. Mar. Chem. 39, 119–149. https://doi.org/10.1016/0304-4203(92)90098-U

Heo, Y., Kim, D.-H., Lee, H., Lee, D., Her, Namguk, J., Yoon, 2016. A new fluorescence index with a fluorescence excitation-emission matrix for dissolved organic matter (DOM) characterization. Desalin. Water Treat. 57, 20270–20282. https://doi.org/10.1080/19443994.2015.1110719

Huguet, A., Vacher, L., Relexans, S., Saubusse, S., Froidefond, J.M., Parlanti, E., 2009. Properties of fluorescent dissolved organic matter in the Gironde Estuary. Org. Geochem. 40, 706–719. https://doi.org/https://doi.org/10.1016/j.orggeochem.2009.03.002

Jaffé, R., Boyer, J.N., Lu, X., Maie, N., Yang, C., Scully, N.M., Mock, S., 2004. Source characterization of dissolved organic matter in a subtropical mangrove-dominated estuary by fluorescence analysis. Mar. Chem. 84, 195–210. https://doi.org/https://doi.org/10.1016/j.marchem.2003.08.001

Kinsey, J.D., Corradino, G., Ziervogel, K., Schnetzer, A., Osburn, C.L., 2018. Formation of Chromophoric Dissolved Organic Matter by Bacterial Degradation of Phytoplankton-

592 Derived Aggregates. Front. Mar. Sci. 4, 430. https://doi.org/10.3389/fmars.2017.00430
593 Kristensen, E., 2000. Organic matter diagenesis at the oxic/anoxic interface in coastal marine
594 sediments, with emphasis on the role of burrowing animals. Hydrobiologia 426, 1–24.
595 https://doi.org/10.1023/A:1003980226194
596 Kuznetsova, O. V, Sevastyanov, V.S., Timerbaev, A.R., 2019. What are the current analytical
597 approaches for sediment analysis related to the study of diagenesis? Highlights from 2010
598 to 2018. Talanta 191, 435–442. https://doi.org/https://doi.org/10.1016/j.talanta.2018.08.080
599 Leeming, R., Nichols, P.D., 1998. Determination of the sources and distribution of sewage and
600 pulp-fibre-derived pollution in the Derwent Estuary, Tasmania, using sterol biomarkers.
601 Mar. Freshw. Res. 49, 7–17. https://doi.org/https://doi.org/10.1071/MF95140
602 Lehmann, M.F., Bernasconi, S.M., Barbieri, A., McKenzie, J.A., 2002. Preservation of organic
603 matter and alteration of its carbon and nitrogen isotope composition during simulated and in
604 situ early sedimentary diagenesis. Geochim. Cosmochim. Acta 66, 3573–3584.
605 https://doi.org/http://dx.doi.org/10.1016/S0016-7037(02)00968-7
606 Li, P., Chen, L., Zhang, W., Huang, Q., 2015. Spatiotemporal Distribution, Sources, and
607 Photobleaching Imprint of Dissolved Organic Matter in the Yangtze Estuary and Its
608 Adjacent Sea Using Fluorescence and Parallel Factor Analysis. PLoS One 10, e0130852.
609 https://doi.org/10.1371/journal.pone.0130852
610 Meyers, P.A., 1994. Preservation of elemental and isotopic source identification of sedimentary
611 organic matter. Chem. Geol. 114, 289–302. https://doi.org/http://dx.doi.org/10.1016/0009-
612 2541(94)90059-0
613 Meyers, P.A., Ishiwatari, R., 1993. Lacustrine organic geochemistry—an overview of indicators
614 of organic matter sources and diagenesis in lake sediments. Org. Geochem. 20, 867–900.

https://doi.org/http://dx.doi.org/10.1016/0146-6380(93)90100-P

Milliken, K.L., 2003. Late Diagenesis and Mass Transfer in Sandstone–Shale Sequences. Treatise on Geochemistry 159–190. https://doi.org/10.1016/B0-08-043751-6/07091-2

Murphy, K.R., Stedmon, C.A., Graeber, D., Bro, R., 2013. Fluorescence spectroscopy and multi-way techniques. PARAFAC. Anal. Methods 5, 6557–6566. https://doi.org/10.1039/C3AY41160E

Navel, S., Mermillod-Blondin, F., Montuelle, B., Chauvet, E., Marmonier, P., 2012. Sedimentary context controls the influence of ecosystem engineering by bioturbators on microbial processes in river sediments. Oikos 121, 1134–1144. https://doi.org/doi:10.1111/j.1600-0706.2011.19742.x

Ogrinc, N., Fontolan, G., Faganeli, J., Covelli, S., 2005. Carbon and nitrogen isotope compositions of organic matter in coastal marine sediments (the Gulf of Trieste, N Adriatic Sea): indicators of sources and preservation. Mar. Chem. 95, 163–181. https://doi.org/http://dx.doi.org/10.1016/j.marchem.2004.09.003

Osburn, C.L., Boyd, T.J., Montgomery, M.T., Bianchi, T.S., Coffin, R.B., Paerl, H.W., 2016a. Optical Proxies for Terrestrial Dissolved Organic Matter in Estuaries and Coastal Waters. Front. Mar. Sci. 2. https://doi.org/10.3389/fmars.2015.00127

Osburn, C.L., Handsel, L.T., Peierls, B.L., Paerl, H.W., 2016b. Predicting Sources of Dissolved Organic Nitrogen to an Estuary from an Agro-Urban Coastal Watershed. Environ. Sci. Technol. 50, 8473–8484. https://doi.org/10.1021/acs.est.6b00053

Pardue, J.W., Scalan, R.S., Van Baalen, C., Parker, P.L., 1976. Maximum carbon isotope fractionation in photosynthesis by blue-green algae and a green alga. Geochim. Cosmochim. Acta 40, 309–312. https://doi.org/https://doi.org/10.1016/0016-7037(76)90208-8

638 Park, M., Snyder, S.A., 2018. Sample handling and data processing for fluorescent excitation-
639 emission matrix (EEM) of dissolved organic matter (DOM). Chemosphere 193, 530–537.
640 https://doi.org/https://doi.org/10.1016/j.chemosphere.2017.11.069
641 Pedrosa-Pàmies, R., Parinos, C., Sanchez-Vidal, A., Gogou, A., Calafat, A., Canals, M.,
642 Bouloubassi, I., Lampadariou, N., 2015. Composition and sources of sedimentary organic
643 matter in the deep eastern Mediterranean Sea. Biogeosciences 12, 7379–7402.
644 https://doi.org/10.5194/bg-12-7379-2015
645 Retelletti Brogi, S., Derrien, M., Hur, J., 2019a. In-Depth Assessment of the Effect of Sodium
646 Azide on the Optical Properties of Dissolved Organic Matter. J. Fluoresc. 1–9.
647 https://doi.org/10.1007/s10895-019-02398-w
648 Retelletti Brogi, S., Kim, J.-H., Ryu, J.-S., Jin, Y.K., Lee, Y.K., Hur, J., 2019b. Exploring
649 sediment porewater dissolved organic matter (DOM) in a mud volcano: Clues of a
650 thermogenic DOM source from fluorescence spectroscopy. Mar. Chem.
651 https://doi.org/10.1016/J.MARCHEM.2019.03.009
652 Shah, V.G.., Dunstan, R.H.., Geary, P.M.., Coombes, P.., Roberts, T.K.., Von Nagy-Felsobuki,
653 E., 2007. Evaluating potential applications of faecal sterols in distinguishing sources of
654 faecal contamination from mixed faecal samples. Water Res. 41, 3691–3700.
655 https://doi.org/10.1016/j.watres.2007.04.006
656 Sillanpää, M., 2015. Natural Organic Matter in Water: Characterization and Treatment Methods,
657 Natural Organic Matter in Water: Characterization and Treatment Methods. Elsevier Inc.
658 https://doi.org/10.1016/C2013-0-19213-6
659 Southwell, M.W., Kieber, R.J., Mead, R.N., Avery, G.B., Skrabal, S.A., 2010. Effects of sunlight
660 on the production of dissolved organic and inorganic nutrients from resuspended sediments.

661 Biogeochemistry 98, 115–126. https://doi.org/10.1007/s10533-009-9380-2
662 Toming, K., Tuvikene, L., Vilbaste, S., Agasild, H., Viik, M., Kisand, A., Feldmann, T., Martma,
663 T., Jones, R.I., Nõges, T., 2013. Contributions of autochthonous and allochthonous sources
664 to dissolved organic matter in a large, shallow, eutrophic lake with a highly calcareous
665 catchment. Limnol. Oceanogr. 58, 1259–1270. https://doi.org/10.4319/lo.2013.58.4.1259
666 van der Meij, W.M., Temme, A.J.A.M., Lin, H.S., Gerke, H.H., Sommer, M., 2018. On the role
667 of hydrologic processes in soil and landscape evolution modeling: concepts, complications
668 and partial solutions. Earth-Science Rev. https://doi.org/10.1016/j.earscirev.2018.09.001
669 Volkman, J.K., 2005. Sterols and other triterpenoids: source specificity and evolution of
670 biosynthetic pathways. Org. Geochem. 36, 139–159.
671 https://doi.org/10.1016/J.ORGGEOCHEM.2004.06.013
672 Volkman, J.K., Tanoue, E., 2002. Chemical and Biological Studies of Particulate Organic Matter
673 in the Ocean. J. Oceanogr. 58, 265–279. https://doi.org/10.1023/a:1015809708632
674 Vonk, J.E., Tank, S.E., Mann, P.J., Spencer, R.G.M., Treat, C.C., Striegl, R.G., Abbott, B.W.,
675 Wickland, K.P., 2015. Biodegradability of dissolved organic carbon in permafrost soils and
676 aquatic systems: a meta-analysis. Biogeosciences 12, 6915–6930.
677 https://doi.org/10.5194/bg-12-6915-2015
678 Wakeham, S.G., Canuel, E.A., 1990. Fatty acids and sterols of particulate matter in a brackish
679 and seasonally anoxic coastal salt pond. Org. Geochem. 16, 703–713.
680 https://doi.org/http://dx.doi.org/10.1016/0146-6380(90)90111-C
681 Waterson, E.J., Canuel, E.A., 2008. Sources of sedimentary organic matter in the Mississippi
682 River and adjacent Gulf of Mexico as revealed by lipid biomarker and δ13CTOC analyses.
683 Org. Geochem. 39, 422–439.

https://doi.org/https://doi.org/10.1016/j.orggeochem.2008.01.011

Wild, B., Andersson, A., Bröder, L., Vonk, J., Hugelius, G., McClelland, J.W., Song, W., Raymond, P.A., Gustafsson, Ö., 2019. Rivers across the Siberian Arctic unearth the patterns of carbon release from thawing permafrost. Proc. Natl. Acad. Sci. U. S. A. 116, 10280–10285. https://doi.org/10.1073/pnas.1811797116

Wünsch, U.J., Murphy, K.R., Stedmon, C.A., 2017. The One-Sample PARAFAC Approach Reveals Molecular Size Distributions of Fluorescent Components in Dissolved Organic Matter. Environ. Sci. Technol. https://doi.org/10.1021/acs.est.7b03260

Xiao, H.-Y., Liu, C.-Q., 2010. Identifying organic matter provenance in sediments using isotopic ratios in an urban river. Geochem. J. 44, 181–187. https://doi.org/10.2343/geochemj.1.0059

Yamashita, Y., Boyer, J.N., Jaffé, R., 2013. Evaluating the distribution of terrestrial dissolved organic matter in a complex coastal ecosystem using fluorescence spectroscopy. Cont. Shelf Res. 66, 136–144. https://doi.org/http://dx.doi.org/10.1016/j.csr.2013.06.010

Yamashita, Y., Maie, N., Briceño, H., Jaffé, R., 2010. Optical characterization of dissolved organic matter in tropical rivers of the Guayana Shield, Venezuela. J. Geophys. Res. Biogeosciences 115, n/a-n/a. https://doi.org/10.1029/2009JG000987

Yu, Z.T., Wang, X.J., Zhang, E.L., Zhao, C.Y., Liu, X.Q., 2015. Spatial distribution and sources of organic carbon in the surface sediment of Bosten Lake, China. Biogeosciences 12, 6605–6615. https://doi.org/10.5194/bg-12-6605-2015

Zhang, L., Yin, K., Wang, L., Chen, F., Zhang, D., Yang, Y., 2009. The sources and accumulation rate of sedimentary organic matter in the Pearl River Estuary and adjacent coastal area, Southern China. Estuar. Coast. Shelf Sci. 85, 190–196. https://doi.org/10.1016/j.ecss.2009.07.035

707 Zhang, Y., Su, Y., Liu, Z., Yu, J., Jin, M., 2017. Lipid biomarker evidence for determining the
708 origin and distribution of organic matter in surface sediments of Lake Taihu, Eastern China.
709 Ecol. Indic. 77, 397–408. https://doi.org/https://doi.org/10.1016/j.ecolind.2017.02.031
710 Zimmerman, A.R., Canuel, E.A., 2001. Bulk Organic Matter and Lipid Biomarker Composition
711 of Chesapeake Bay Surficial Sediments as Indicators of Environmental Processes. Estuar.
712 Coast. Shelf Sci. 53, 319–341. https://doi.org/http://dx.doi.org/10.1006/ecss.2001.0815
713 Zsolnay, A., Baigar, E., Jimenez, M., Steinweg, B., Saccomandi, F., 1999. Differentiating with
714 fluorescence spectroscopy the sources of dissolved organic matter in soils subjected to
715 drying. Chemosphere 38, 45–50. https://doi.org/http://dx.doi.org/10.1016/S0045-
716 6535(98)00166-0
717

Figure 1. Relative abundances (%) of the four different fluorescent components (C1–C4) in the artificial sediments at five different mixing ratios of two end-members (i.e., soil and algae) under oxic and anoxic conditions at the incubation time of 0 and 60 days. The lines and dashed lines represent the evolution of the parameters with varying mixing ratios of the two end-members.

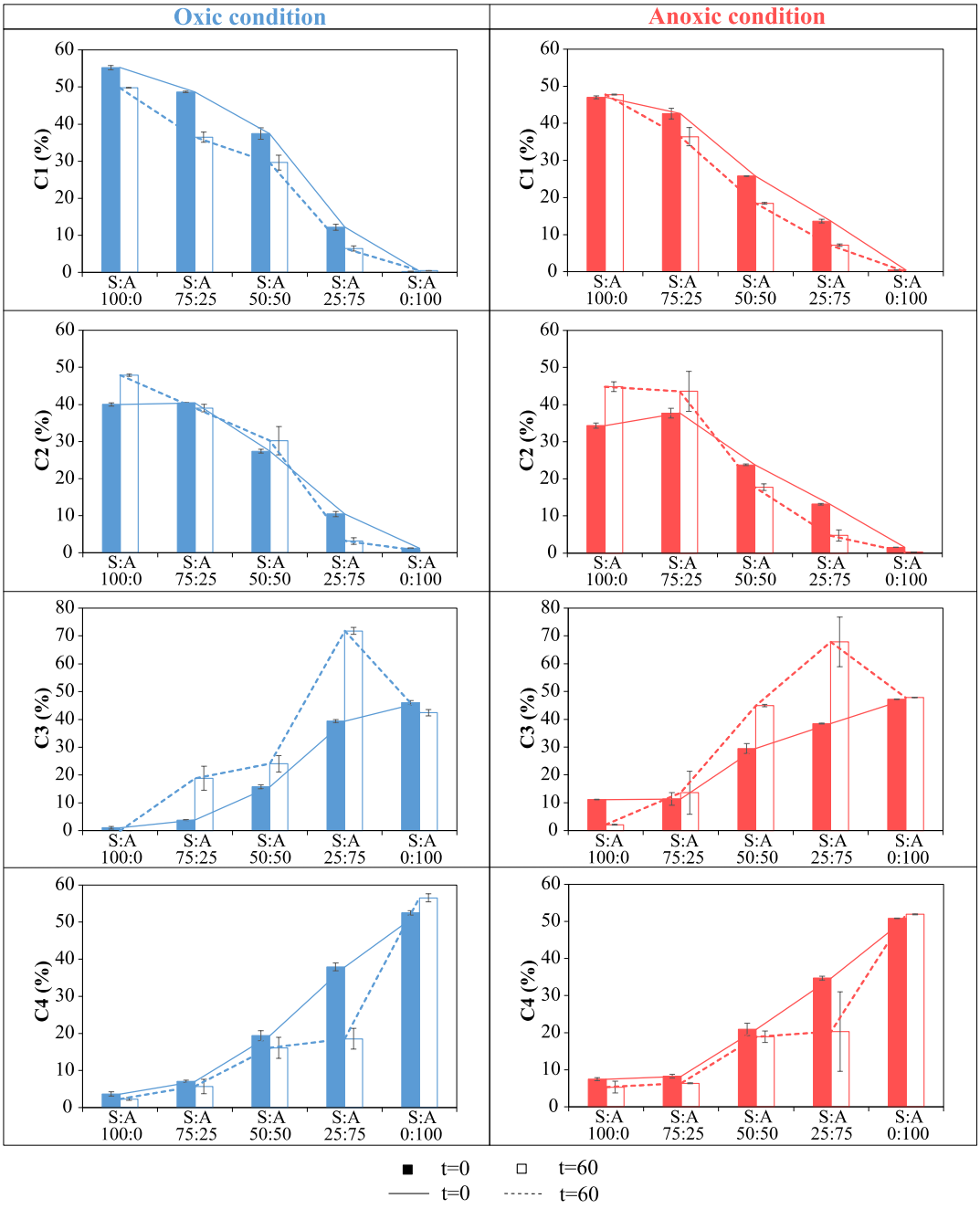

Figure 2. Values of the absorbance and fluorescent indices SUVA (a), FI (b), YFI (c), HIX (d), and BIX (e) in the artificial sediments at five different mixing ratios of two end-members (i.e., soil and algae) under oxic and anoxic conditions at the incubation time of 0 and 60 days. The blue color is used for the data of oxic conditions while pink color for those of anoxic conditions.

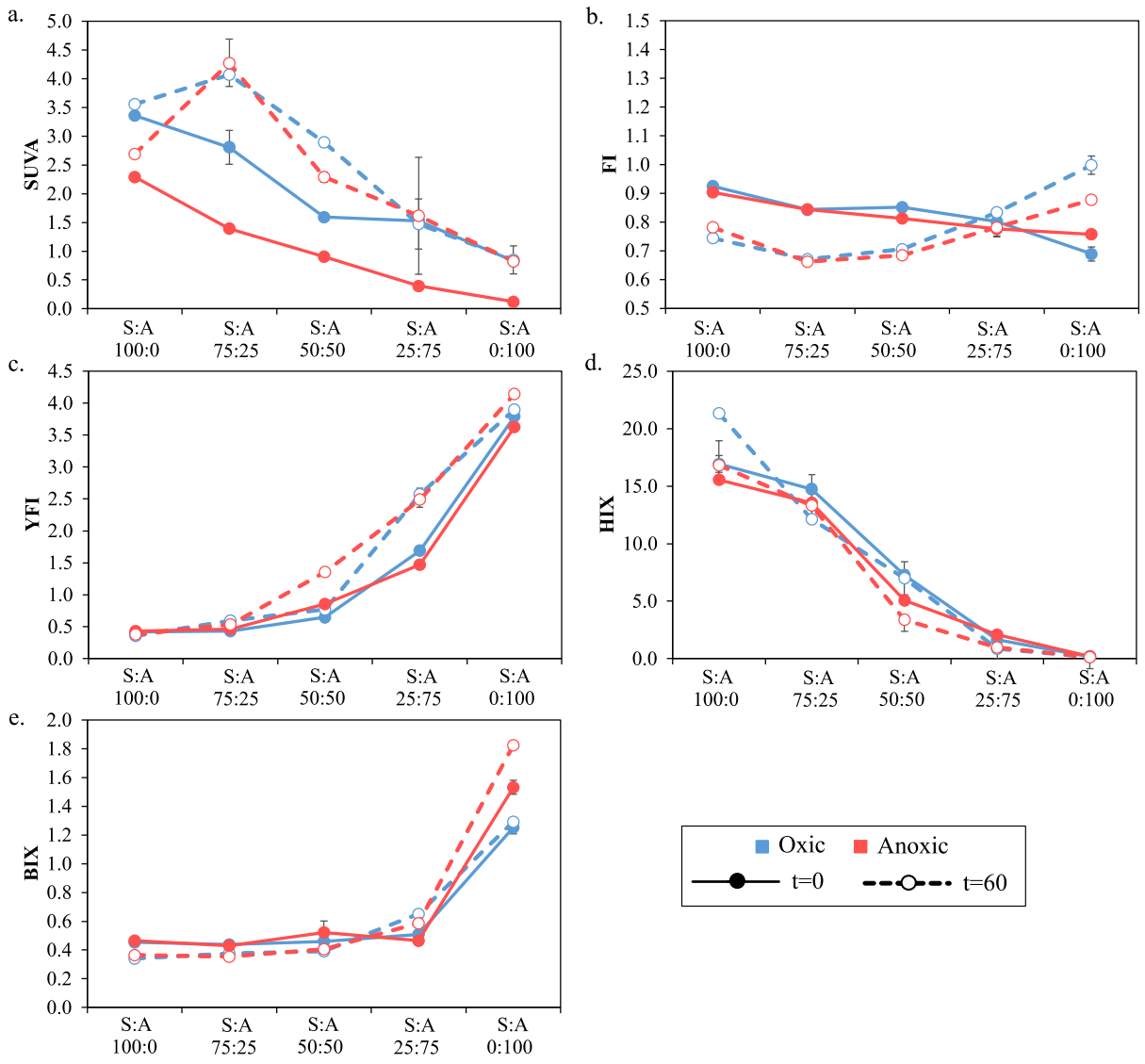

Figure 3. Values of the carbon stable isotopes in the artificial sediments at five different mixing ratios of two end-members (i.e., soil and algae) under oxic and anoxic conditions at the incubation time of 0 and 60 days. The blue color is used for the data of oxic conditions while pink color for those of anoxic conditions.

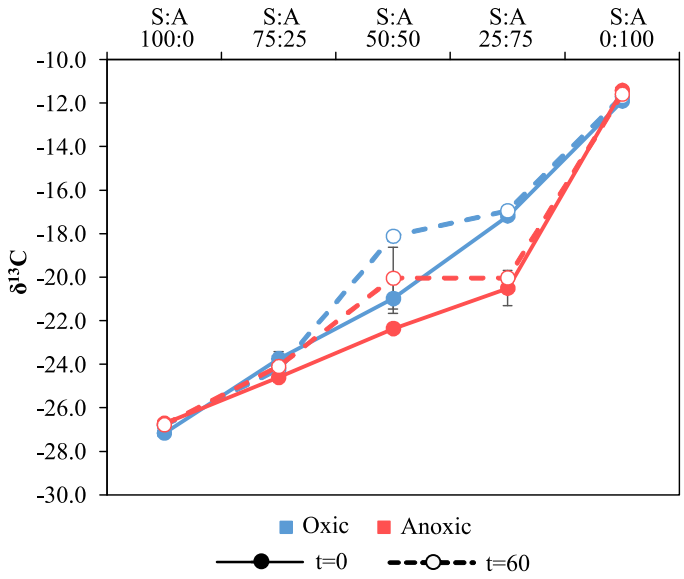

Figure 4. Relative abundances (%) of the seven sterols/stanols in the artificial sediments at five different mixing ratios of two end-members (i.e., soil and algae) under oxic and anoxic conditions at the incubation time of 0 and 60 days. The lines and dashed lines represent the evolution of the parameters with varying mixing ratios of the two end-members.

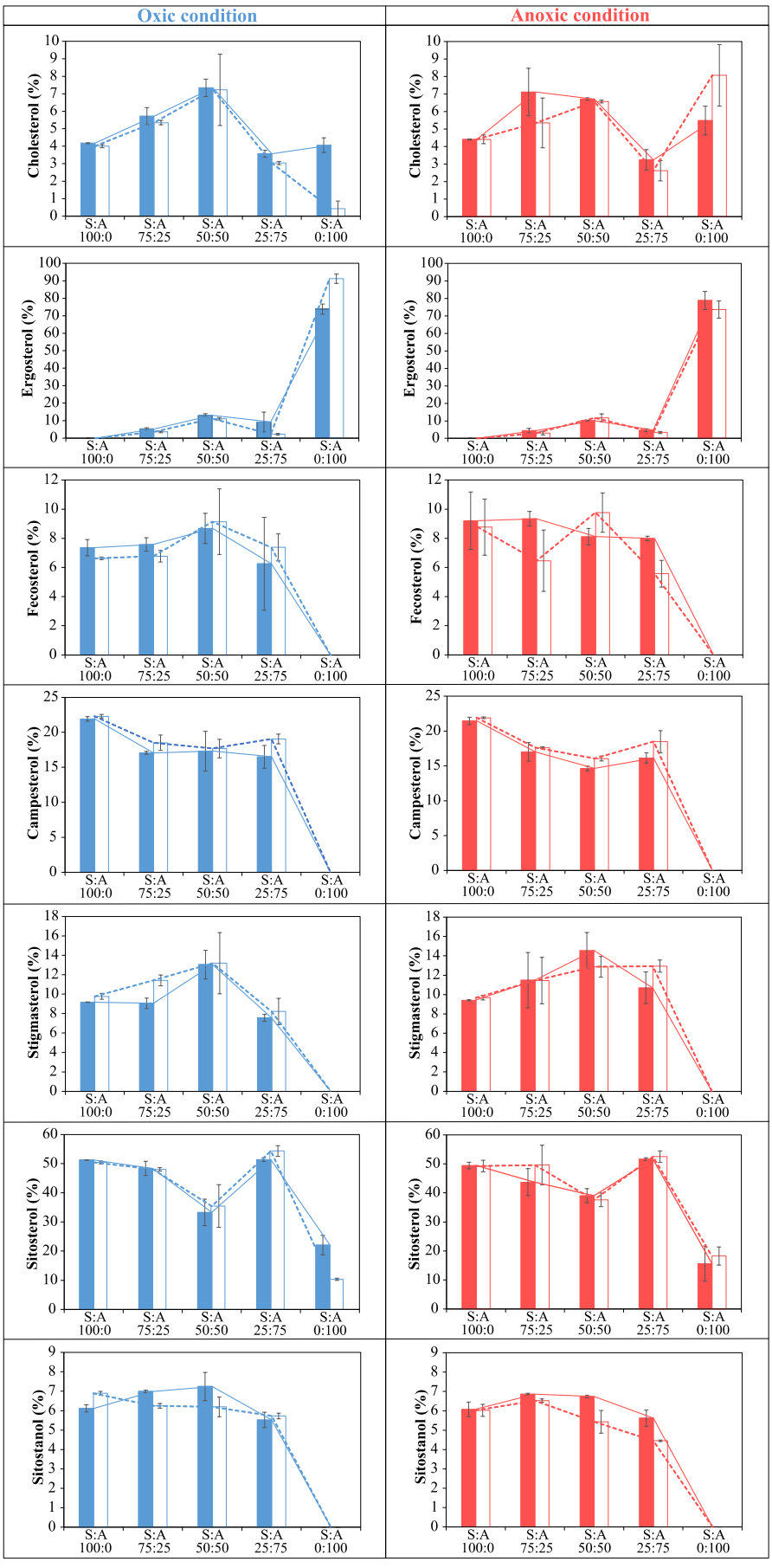
Oxic condition
Anoxic condition
Cholesterol (%)
Ergosterol (%)
Fecosterol (%)
Campesterol (%)
Stigmasterol (%)
Sitosterol (%)
Sitostanol (%)
S:A 100:0
S:A 75:25
S:A 50:50
S:A 25:75
S:A 0:100
t=0
t=60
t=0
t=60

Table 1. The relative changes of the 4 identified components (%) and the spectroscopic indices, the carbon stable isotopic ratios (‰) and the distribution in the sterols/stanols in the artificial sediment of the two end-members before versus after incubation under oxic and anoxic conditions (average values ± standard deviation).

		Soil end-member				**Algae end-member**			
		Oxic		Anoxic		Oxic		Anoxic	
		0 day-incubation	60 days-incubation	0 day-incubation	60 days-incubation	0 day-incubation	60 days-incubation	0 day-incubation	60 days-incubation
Absorbance and fluorescence proxies	C1 (%)	55.2 ± 0.6	49.8 ± 0.1	47.0 ± 0.4	47.7 ± 0.1	0.3 ± 0.1	0.5 ± 0.0	0.5 ± 0.0	0.0 ± 0.0
	C2 (%)	40.0 ± 0.4	47.9 ± 0.3	34.4 ± 0.7	44.8 ± 1.3	1.2 ± 0.1	0.6 ± 0.0	1.5 ± 0.0	0.2 ± 0.0
	C3 (%)	1.1 ± 0.5	0.0 ± 0.0	11.2 ± 0.1	2.1 ± 0.1	46.0 ± 0.8	42.4 ± 1.1	47.2 ± 0.1	47.8 ± 0.1
	C4 (%)	3.7 ± 0.5	2.3 ± 0.3	7.5 ± 0.4	5.3 ± 1.6	52.5 ± 0.6	56.5 ± 1.1	50.8 ± 0.1	51.9 ± 0.1
	$SUVA_{254}$ ($L.mg^{-1}.m^{-1}$)	3.4 ± 0.1	3.6 ± 0.1	2.3 ± 0.0	2.7 ± 0.1	0.8 ± 0.1	0.8 ± 0.2	0.1 ± 0.0	0.8 ± 0.0
	FI	0.9 ± 0.0	0.7 ± 0.0	0.9 ± 0.0	0.8 ± 0.0	0.7 ± 0.0	1.0 ± 0.0	0.8 ± 0.0	0.9 ± 0.0
	YFI	0.4 ± 0.0	0.4 ± 0.0	0.4 ± 0.0	0.4 ± 0.0	3.8 ± 0.0	3.9 ± 0.0	3.6 ± 0.0	4.1 ± 0.0
	HIX	16.9 ± 0.7	21.3 ± 0.2	15.6 ± 0.4	16.8 ± 2.1	0.2 ± 0.0	0.2 ± 0.0	0.2 ± 0.0	0.1 ± 0.0
	BIX	0.5 ± 0.0	0.3 ± 0.0	0.5 ± 0.0	0.4 ± 0.0	1.3 ± 0.0	1.3 ± 0.0	1.5 ± 0.0	1.8 ± 0.0
Isotopes	$\delta^{13}C$ (‰)	-27.2 ± 0.1	-26.8 ± 0.1	-26.7 ± 0.1	-26.8 ± 0.1	-11.9 ± 0.0	-11.7 ± 0.0	-11.4 ± 0.1	-11.6 ± 0.1
Sterols/stanols	Cholesterol (%)	4.2 ± 0.0	4.0 ± 0.1	4.4 ± 0.0	4.4 ± 0.2	4.1 ± 0.4	0.4 ± 0.4	5.5 ± 0.8	8.1 ± 1.8
	Ergosterol (%)	0.0 ± 0.0	0.0 ± 0.0	0.0 ± 0.0	0.0 ± 0.0	73.9 ± 2.9	91.1 ± 2.7	78.9 ± 5.2	73.6 ± 4.9
	Fecosterol (%)	7.4 ± 0.6	6.6 ± 0.1	9.2 ± 2.0	8.8 ± 1.9	0.0 ± 0.0	0.0 ± 0.0	0.0 ± 0.0	0.0 ± 0.0
	Campesterol (%)	21.9 ± 0.3	22.3 ± 0.3	21.5 ± 0.5	21.9 ± 0.1	0.0 ± 0.0	0.0 ± 0.0	0.0 ± 0.0	0.0 ± 0.0
	Stigmasterol (%)	9.2 ± 0.0	9.8 ± 0.3	9.4 ± 0.0	9.7 ± 0.2	0.0 ± 0.0	0.0 ± 0.0	0.0 ± 0.0	0.0 ± 0.0
	Sitosterol (%)	51.3 ± 0.1	50.4 ± 0.5	49.1 ± 1.1	49.2 ± 2.0	22.1 ± 3.3	10.3 ± 0.4	15.6 ± 6.0	18.3 ± 3.1
	Sitostanol (%)	6.1 ± 0.2	6.9 ± 0.1	6.1 ± 0.4	6.0 ± 0.3	0.0 ± 0.0	0.0 ± 0.0	0.0 ± 0.0	0.0 ± 0.0

Table 2. The evaluation of selected source discrimination indices in the relationships with increasing algal carbon fraction (% Algae) of the artificial sediments at 0-day incubation.

Parameters	Oxygen condition	Tendency	Relationship type[a]	R^2 (*p*-value)	S_m[b]	S_m/SD[c]	S_p[d]	% difference[e]	Applicability[f]
Extractable OM									
C1 (%)	Oxic	↓	Linear	**0.958 (<0.01)**	0.585	**0.905**	0.550	**6.5**	**OOO**
	Anoxic	↓	Linear	**0.979 (<0.01)**	0.488	**0.992**	0.465	**4.9**	**OOO**
C2 (%)	Oxic	↓	Linear	**0.933 (<0.01)**	0.430	**1.159**	0.388	10.9	**OOX**
	Anoxic	↓	Linear	**0.904 (<0.01)**	0.361	**0.752**	0.328	**9.9**	**OOO**
C3 (%)	Oxic	↑	Linear	**0.935 (<0.01)**	0.501	**0.917**	0.449	11.7	**OOX**
	Anoxic	↑	Linear	**0.946 (<0.01)**	0.397	0.443	0.360	10.1	OXX
C4 (%)	Oxic	↑	Linear	**0.956 (<0.01)**	0.514	**0.668**	0.488	**5.3**	**OOO**
	Anoxic	↑	Linear	**0.939 (<0.01)**	0.452	**0.713**	0.433	**4.4**	**OOO**
SUVA254 ($L.mg^{-1}.m^{-1}$)	Oxic	↓	Linear	**0.944 (<0.01)**	0.025	0.258	0.025	0.3	OXX
	Anoxic	↓	Linear	**0.961 (<0.01)**	0.021	**1.433**	0.022	**1.6**	**OOO**
FI	Oxic	↓	Linear	**0.877** (0.019)	0.002	0.290	0.002	13.0	OXX
	Anoxic	↓	Linear	**0.964 (<0.01)**	0.001	0.137	0.001	**1.5**	**OXO**
YFI	Oxic	↑	Nonlinear	0.775 (0.049)	0.032	**1.419**	0.034	**5.0**	**XOO**
	Anoxic	↑	Nonlinear	0.774 (0.049)	0.030	**3.006**	0.032	**7.4**	**XOO**
HIX	Oxic	↓	Linear	**0.956 (<0.01)**	0.186	**0.551**	0.168	11.3	**OOX**
	Anoxic	↓	Linear	**0.937 (<0.01)**	0.169	0.471	0.154	**9.9**	**OXO**
BIX	Oxic	↑	Nonlinear	0.558 (0.147)	0.007	0.361	0.008	16.5	XXX
	Anoxic	↑	Nonlinear	0.519 (0.170)	0.009	0.262	0.011	18.7	XXX
$\delta^{13}C$ (‰)	Oxic	↑	Linear	**0.985 (<0.01)**	0.148	**0.660**	0.153	**2.8**	**OOO**
	Anoxic	↑	Linear	**0.863** (0.023)	0.139	0.481	0.153	**9.3**	**OXO**
Cholesterol (%)	Oxic	↓	Nonlinear	0.059 (0.694)	0.010	0.029	0.001	726.5	XXX
	Anoxic	↓	Nonlinear	0.028 (0.787)	0.007	0.012	0.011	163.2	XXX
Ergosterol (%)	Oxic	↑	Nonlinear	0.625 (0.111)	0.607	0.299	0.739	17.8	XXX
	Anoxic	↑	Nonlinear	0.562 (0.144)	0.632	0.418	0.789	19.9	XXX
Fecosterol (%)	Oxic	↓	Nonlinear	0.541 (0.157)	0.064	0.061	0.074	12.8	XXX
	Anoxic	↓	Nonlinear	0.635 (0.107)	0.079	0.123	0.092	14.1	XXX
Campesterol (%)	Oxic	↓	Nonlinear	0.695 (0.079)	0.178	0.179	0.219	19.0	XXX
	Anoxic	↓	Nonlinear	0.722 (0.068)	0.175	0.300	0.215	18.4	XXX

Stigmasterol (%)	Oxic	↓	Nonlinear	0.429 (0.230)	0.079	0.167	0.092	13.5	XXX
	Anoxic	↓	Nonlinear	0.319 (0.321)	0.079	0.061	0.094	16.6	XXX
Sitosterol (%)	Oxic	↓	Nonlinear	0.447 (0.217)	0.221	0.101	0.292	24.1	XXX
	Anoxic	↓	Nonlinear	0.428 (0.231)	0.239	0.080	0.338	29.4	XXX
Sitostanol (%)	Oxic	↓	Nonlinear	0.530 (0.163)	0.055	0.200	0.061	10.4	XXX
	Anoxic	↓	Nonlinear	0.544 (0.155)	0.054	0.296	0.061	11.8	XXX

[a]: The relationship is considered linear for $R^2 > 0.8$ with a *p*-value < 0.01.

[b]: The absolute value of the regression slope for the measured values.

[c]: The absolute value of the regression slope for the measured values divided by the average standard deviation of the measurement. A value of the S_m/SD superior to 1.0 was considered as an acceptable sensitivity in the source discrimination relative to the measurement uncertainty

[d]: The absolute value of the regression slope for the predicted values (e.g., data presented in Table S2).

[e]: The difference (%) between the slope of the measured and predicted values. A difference of < 10% is considered an acceptable deviation. The value of 10% was arbitrarily chosen by the authors.

[f]: The applicability is evaluated via the criteria based on R^2, S_m/SD, and % difference. O means the value of the standard respect the critical value while X the indices failed (e.g., Critical values for R^2 and an associated p-value of R^2, S_m/SD and % difference are > 0.8 and < 0.01, > 0.5, and < 10%, respectively).

Table 3. The evaluation of selected source discrimination indices in the relationships with increasing algal carbon fraction (% Algae) of the artificial sediments at 60-days incubation.

Parameters	Oxygen condition	Tendency	Relationship type[a]	R^2 (*p*-value)	S_m[b]	S_m/SD[c]	S_p[d]	% difference[e]	Applicability[f]
Extractable OM									
C1 (%)	Oxic	↓	Linear	**0.967 (<0.01)**	0.514	**0.614**	0.493	**4.4**	**OOO**
	Anoxic	↓	Linear	**0.980 (<0.01)**	0.499	**0.795**	0.477	**4.5**	**OOO**
C2 (%)	Oxic	↓	Linear	**0.937 (<0.01)**	0.522	0.439	0.473	10.3	OXX
	Anoxic	↓	Linear	**0.922 (<0.01)**	0.512	0.281	0.446	14.9	OXX
C3 (%)	Oxic	↑	Linear	0.643 (0.103)	0.551	0.284	0.424	30.0	XXX
	Anoxic	↑	Linear	0.737 (0.063)	0.582	0.168	0.457	27.5	XXX
C4 (%)	Oxic	↑	Linear	0.787 (0.045)	0.485	0.268	0.542	10.5	XXX
	Anoxic	↑	Linear	**0.809** (0.038)	0.429	0.152	0.466	**8.0**	**OXO**
SUVA254 ($L.mg^{-1}.m^{-1}$)	Oxic	↓	Linear	**0.856** (0.024)	0.032	0.192	0.027	18.4	OXX
	Anoxic	↓	Nonlinear	0.611 (0.118)	0.026	0.080	0.019	36.9	XXX
FI	Oxic	↑	Nonlinear	0.654 (0.097)	0.003	0.200	0.003	**5.7**	XXO
	Anoxic	↑	Nonlinear	0.321 (0.319)	0.001	0.112	0.001	29.8	XXX
YFI	Oxic	↑	Linear	**0.867** (0.021)	0.036	**0.682**	0.035	**2.3**	**OOO**
	Anoxic	↑	Linear	**0.919 (<0.01)**	0.038	**0.688**	0.038	**0.8**	**OOO**
HIX	Oxic	↓	Linear	**0.934 (<0.01)**	0.214	**0.542**	0.212	**1.3**	**OOO**
	Anoxic	↓	Linear	**0.898** (0.014)	0.183	0.169	0.167	**9.5**	**OXO**
BIX	Oxic	↑	Nonlinear	0.739 (0.062)	0.009	**0.534**	0.010	**8.5**	XOX
	Anoxic	↑	Nonlinear	0.622 (0.113)	0.013	**1.202**	0.015	13.6	XOX
$\delta^{13}C$ (‰)	Oxic	↑	Linear	**0.969 (<0.01)**	0.150	**1.431**	0.151	**0.7**	**OOO**
	Anoxic	↑	Nonlinear	**0.898** (0.014)	0.138	0.274	0.152	**9.3**	**OXO**
Cholesterol (%)	Oxic	↓	Nonlinear	0.346 (0.297)	0.038	0.068	0.036	**5.8**	XXO
	Anoxic	↓	Nonlinear	0.123 (0.563)	0.018	0.022	0.037	49.8	XXX
Ergosterol (%)	Oxic	↑	Nonlinear	0.536 (0.160)	0.724	**0.835**	0.911	20.6	XOX
	Anoxic	↑	Nonlinear	0.560 (0.146)	0.591	0.335	0.736	19.8	XXX
Fecosterol (%)	Oxic	↓	Nonlinear	0.328 (0.313)	0.051	0.069	0.066	23.7	XXX
	Anoxic	↓	Nonlinear	0.591 (0.129)	0.074	0.059	0.088	16.0	XXX
Campesterol (%)	Oxic	↓	Nonlinear	0.620 (0.114)	0.176	0.262	0.223	21.0	XXX
	Anoxic	↓	Nonlinear	0.630 (0.109)	0.172	0.392	0.219	21.6	XXX

Stigmasterol (%)	Oxic	↓	Nonlinear	0.495 (0.185)	0.091	0.084	0.098	**6.9**	XXO
	Anoxic	↓	Nonlinear	0.272 (0.367)	0.071	0.082	0.097	26.2	XXX
Sitosterol (%)	Oxic	↓	Nonlinear	0.427 (0.232)	0.296	0.140	0.401	26.3	XXX
	Anoxic	↓	Nonlinear	0.434 (0.227)	0.236	0.073	0.309	23.8	XXX
Sitostanol (%)	Oxic	↓	Nonlinear	0.638 (0.105)	0.057	0.328	0.069	17.0	XXX
	Anoxic	↓	Nonlinear	0.723 (0.068)	0.056	0.278	0.060	**6.2**	XXO

[a]: The relationship is considered linear for $R^2 > 0.8$ with a *p*-value < 0.01.

[b]: The absolute value of the regression slope for the measured values.

[c]: The absolute value of the regression slope for the measured values divided by the average standard deviation of the measurement. A value of the S_m/SD superior to 1.0 was considered as an acceptable sensitivity in the source discrimination relative to the measurement uncertainty

[d]: The absolute value of the regression slope for the predicted values (e.g., data presented in Table S2).

[e]: The difference (%) between the slope of the measured and predicted values. A difference of < 10% is considered an acceptable deviation.

[f]: The applicability is evaluated via the criteria based on R^2, S_m/SD, and % difference. O means the value of the standard respect the critical value while X the indices failed (e.g., Critical values for R^2 and an associated p-value of R^2, S_m/SD and % difference are > 0.8 and < 0.01, > 0.5, and < 10%, respectively).